

Precise Measurement of the Neutrino Mixing Parameter θ_{23} from Muon Neutrino Disappearance in an Off-Axis Beam

K. Abe,⁴⁶ J. Adam,³² H. Aihara,^{45,23} T. Akiri,⁹ C. Andreopoulos,⁴⁴ S. Aoki,²⁴ A. Ariga,² T. Ariga,² S. Assylbekov,⁸ D. Autiero,²⁹ M. Barbi,³⁹ G.J. Barker,⁵⁴ G. Barr,³⁵ M. Bass,⁸ M. Batkiewicz,¹³ F. Bay,¹¹ S.W. Bentham,²⁶ V. Berardi,¹⁸ B.E. Berger,⁸ S. Berkman,⁴ I. Bertram,²⁶ S. Bhadra,⁵⁸ F.d.M. Blaszczyk,²⁸ A. Blondel,¹² C. Bojchko,⁵¹ S. Bordini,¹⁵ S.B. Boyd,⁵⁴ D. Brailsford,¹⁷ A. Bravar,¹² C. Bronner,²⁵ N. Buchanan,⁸ R.G. Calland,²⁷ J. Caravaca Rodríguez,¹⁵ S.L. Cartwright,⁴² R. Castillo,¹⁵ M.G. Catanesi,¹⁸ A. Cervera,¹⁶ D. Cherdack,⁸ G. Christodoulou,²⁷ A. Clifton,⁸ J. Coleman,²⁷ S.J. Coleman,⁷ G. Collazuol,²⁰ K. Connolly,⁵⁵ L. Cremonesi,³⁸ A. Dabrowska,¹³ I. Danko,³⁷ R. Das,⁸ S. Davis,⁵⁵ P. de Perio,⁴⁹ G. De Rosa,¹⁹ T. Dealtry,^{44,35} S.R. Dennis,^{54,44} C. Densham,⁴⁴ F. Di Lodovico,³⁸ S. Di Luise,¹¹ O. Drapier,¹⁰ T. Dubowski,³⁸ K. Duffy,³⁵ F. Dufour,¹² J. Dumarchez,³⁶ S. Dytman,³⁷ M. Dziewiecki,⁵³ S. Emery,⁶ A. Ereditato,² L. Escudero,¹⁶ A.A.J. Finch,²⁶ L. Floetotto,⁴¹ M. Friend,^{14,*} Y. Fujii,^{14,*} Y. Fukuda,³⁰ A.P. Furmanski,⁵⁴ V. Galymov,⁶ S. Giffin,³⁹ C. Giganti,³⁶ K. Gilje,³² D. Goeldi,² T. Golan,⁵⁷ M. Gonin,¹⁰ N. Grant,²⁶ D. Gudin,²² D.R. Hadley,⁵⁴ A. Haesler,¹² M.D. Haigh,⁵⁴ P. Hamilton,¹⁷ D. Hansen,³⁷ T. Hara,²⁴ M. Hartz,^{23,50} T. Hasegawa,^{14,*} N.C. Hastings,³⁹ Y. Hayato,⁴⁶ C. Hearty,^{4,†} R.L. Helmer,⁵⁰ M. Hierholzer,² J. Hignight,³² A. Hillairet,⁵¹ A. Himmel,⁹ T. Hiraki,²⁵ S. Hirota,²⁵ J. Holeczek,⁴³ S. Horikawa,¹¹ K. Huang,²⁵ A.K. Ichikawa,²⁵ K. Ieki,²⁵ M. Ieva,¹⁵ M. Ikeda,⁴⁶ J. Imber,³² J. Insler,²⁸ T.J. Irvine,⁴⁷ T. Ishida,^{14,*} T. Ishii,^{14,*} S.J. Ives,¹⁷ E. Iwai,¹⁴ K. Iyogi,⁴⁶ A. Izmaylov,^{16,22} A. Jacob,³⁵ B. Jamieson,⁵⁶ R.A. Johnson,⁷ J.H. Jo,³² P. Jonsson,¹⁷ C.K. Jung,^{32,‡} M. Kabirnezhad,³¹ A.C. Kaboth,¹⁷ T. Kajita,^{47,‡} H. Kakuno,⁴⁸ J. Kameda,⁴⁶ Y. Kanazawa,⁴⁵ D. Karlen,^{51,50} I. Karpikov,²² E. Kearns,^{3,23,‡} M. Khabibullin,²² A. Khotjantsev,²² D. Kielczewska,⁵² T. Kikawa,²⁵ A. Kilinski,³¹ J. Kim,⁴ J. Kisiel,⁴³ P. Kitching,¹ T. Kobayashi,^{14,*} L. Koch,⁴¹ A. Kolaceke,³⁹ A. Konaka,⁵⁰ L.L. Kormos,²⁶ A. Korzenev,¹² K. Koseki,^{14,*} Y. Koshio,^{33,‡} I. Kreslo,² W. Kropp,⁵ H. Kubo,²⁵ Y. Kudenko,^{22,§} S. Kumaratunga,⁵⁰ R. Kurjata,⁵³ T. Kutter,²⁸ J. Lagoda,³¹ K. Laihem,⁴¹ I. Lamont,²⁶ M. Laveder,²⁰ M. Lawe,⁴² M. Lazos,²⁷ K.P. Lee,⁴⁷ T. Lindner,⁵⁰ C. Lister,⁵⁴ R.P. Litchfield,⁵⁴ A. Longhin,²⁰ L. Ludovici,²¹ M. Macaire,⁶ L. Magaletti,¹⁸ K. Mahn,⁵⁰ M. Malek,¹⁷ S. Manly,⁴⁰ A.D. Marino,⁷ J. Marteau,²⁹ J.F. Martin,⁴⁹ T. Maruyama,^{14,*} J. Marzec,⁵³ E.L. Mathie,³⁹ V. Matveev,²² K. Mavrokoridis,²⁷ E. Mazzucato,⁶ M. McCarthy,⁴ N. McCauley,²⁷ K.S. McFarland,⁴⁰ C. McGrew,³² C. Metelko,²⁷ M. Mezzetto,²⁰ P. Mijakowski,³¹ C.A. Miller,⁵⁰ A. Minamino,²⁵ O. Mineev,²² S. Mine,⁵ A. Missert,⁷ M. Miura,^{46,‡} L. Monfregola,¹⁶ S. Moriyama,^{46,‡} Th.A. Mueller,¹⁰ A. Murakami,²⁵ M. Murdoch,²⁷ S. Murphy,¹¹ J. Myslik,⁵¹ T. Nagasaki,²⁵ T. Nakadaira,^{14,*} M. Nakahata,^{46,23} T. Nakai,³⁴ K. Nakamura,^{23,14,*} S. Nakayama,^{46,‡} T. Nakaya,^{25,23} K. Nakayoshi,^{14,*} D. Naples,³⁷ C. Nielsen,⁴ M. Nirkko,² K. Nishikawa,^{14,*} Y. Nishimura,⁴⁷ H.M. O'Keefe,²⁶ R. Ohta,^{14,*} K. Okumura,^{47,23} T. Okusawa,³⁴ W. Orszyszczak,⁵² S.M. Oser,⁴ R.A. Owen,³⁸ Y. Oyama,^{14,*} V. Palladino,¹⁹ J. Palomino,³² V. Paolone,³⁷ D. Payne,²⁷ O. Perevozchikov,²⁸ J.D. Perkin,⁴² Y. Petrov,⁴ L. Pickard,⁴² E.S. Pinzon Guerra,⁵⁸ C. Pistillo,² P. Plonski,⁵³ E. Poplawska,³⁸ B. Popov,^{36,¶} M. Posiadala,⁵² J.-M. Poutissou,⁵⁰ R. Poutissou,⁵⁰ P. Przewlocki,³¹ B. Quilain,¹⁰ E. Radicioni,¹⁸ P.N. Ratoff,²⁶ M. Ravonel,¹² M.A.M. Rayner,¹² A. Redij,² M. Reeves,²⁶ E. Reinherz-Aronis,⁸ F. Retiere,⁵⁰ A. Robert,³⁶ P.A. Rodrigues,⁴⁰ P. Rojas,⁸ E. Rondio,³¹ S. Roth,⁴¹ A. Rubbia,¹¹ D. Ruterbories,⁸ R. Sacco,³⁸ K. Sakashita,^{14,*} F. Sánchez,¹⁵ F. Sato,¹⁴ E. Scantamburlo,¹² K. Scholberg,^{9,‡} S. Schoppmann,⁴¹ J. Schwehr,⁸ M. Scott,⁵⁰ Y. Seiya,³⁴ T. Sekiguchi,^{14,*} H. Sekiya,^{46,‡} D. Sgalaberna,¹¹ M. Shiozawa,^{46,23} S. Short,¹⁷ Y. Shustrov,²² P. Sinclair,¹⁷ B. Smith,¹⁷ R.J. Smith,³⁵ M. Smy,⁵ J.T. Sobczyk,⁵⁷ H. Sobel,^{5,23} M. Sorel,¹⁶ L. Southwell,²⁶ P. Stamoulis,¹⁶ J. Steinmann,⁴¹ B. Still,³⁸ Y. Suda,⁴⁵ A. Suzuki,²⁴ K. Suzuki,²⁵ S.Y. Suzuki,^{14,*} Y. Suzuki,^{46,23} T. Szegłowski,⁴³ R. Tacik,^{39,50} M. Tada,^{14,*} S. Takahashi,²⁵ A. Takeda,⁴⁶ Y. Takeuchi,^{24,23} H.K. Tanaka,^{46,‡} H.A. Tanaka,^{4,†} M.M. Tanaka,^{14,*} D. Terhorst,⁴¹ R. Terri,³⁸ L.F. Thompson,⁴² A. Thorley,²⁷ S. Tobayama,⁴ W. Toki,⁸ T. Tomura,⁴⁶ Y. Totsuka,^{**} C. Touramanis,²⁷ T. Tsukamoto,^{14,*} M. Tzanov,²⁸ Y. Uchida,¹⁷ K. Ueno,⁴⁶ A. Vacheret,³⁵ M. Vagins,^{23,5} G. Vasseur,⁶ T. Wachala,¹³ A.V. Waldron,³⁵ C.W. Walter,^{9,‡} D. Wark,^{44,17} M.O. Wascko,¹⁷ A. Weber,^{44,35} R. Wendell,^{46,‡} R.J. Wilkes,⁵⁵ M.J. Wilking,⁵⁰ C. Wilkinson,⁴² Z. Williamson,³⁵ J.R. Wilson,³⁸ R.J. Wilson,⁸ T. Wongjirad,⁹ Y. Yamada,^{14,*} K. Yamamoto,³⁴ C. Yanagisawa,^{32,††} S. Yen,⁵⁰ N. Yershov,²² M. Yokoyama,^{45,‡} T. Yuan,⁷ M. Yu,⁵⁸ A. Zalewska,¹³ J. Zalipska,³¹ L. Zambelli,³⁶ K. Zaremba,⁵³ M. Ziembicki,⁵³ E.D. Zimmerman,⁷ M. Zito,⁶ and J. Żmuda⁵⁷

(The T2K Collaboration)

¹University of Alberta, Centre for Particle Physics, Department of Physics, Edmonton, Alberta, Canada

²University of Bern, Albert Einstein Center for Fundamental Physics, Laboratory for High Energy Physics (LHEP), Bern, Switzerland

³Boston University, Department of Physics, Boston, Massachusetts, U.S.A.

- ⁴University of British Columbia, Department of Physics and Astronomy, Vancouver, British Columbia, Canada
- ⁵University of California, Irvine, Department of Physics and Astronomy, Irvine, California, U.S.A.
- ⁶IRFU, CEA Saclay, Gif-sur-Yvette, France
- ⁷University of Colorado at Boulder, Department of Physics, Boulder, Colorado, U.S.A.
- ⁸Colorado State University, Department of Physics, Fort Collins, Colorado, U.S.A.
- ⁹Duke University, Department of Physics, Durham, North Carolina, U.S.A.
- ¹⁰Ecole Polytechnique, IN2P3-CNRS, Laboratoire Leprince-Ringuet, Palaiseau, France
- ¹¹ETH Zurich, Institute for Particle Physics, Zurich, Switzerland
- ¹²University of Geneva, Section de Physique, DPNC, Geneva, Switzerland
- ¹³H. Niewodniczanski Institute of Nuclear Physics PAN, Cracow, Poland
- ¹⁴High Energy Accelerator Research Organization (KEK), Tsukuba, Ibaraki, Japan
- ¹⁵Institut de Fisica d'Altes Energies (IFAE), Bellaterra (Barcelona), Spain
- ¹⁶IFIC (CSIC & University of Valencia), Valencia, Spain
- ¹⁷Imperial College London, Department of Physics, London, United Kingdom
- ¹⁸INFN Sezione di Bari and Università e Politecnico di Bari, Dipartimento Interuniversitario di Fisica, Bari, Italy
- ¹⁹INFN Sezione di Napoli and Università di Napoli, Dipartimento di Fisica, Napoli, Italy
- ²⁰INFN Sezione di Padova and Università di Padova, Dipartimento di Fisica, Padova, Italy
- ²¹INFN Sezione di Roma and Università di Roma "La Sapienza", Roma, Italy
- ²²Institute for Nuclear Research of the Russian Academy of Sciences, Moscow, Russia
- ²³Kavli Institute for the Physics and Mathematics of the Universe (WPI),
Todai Institutes for Advanced Study, University of Tokyo, Kashiwa, Chiba, Japan
- ²⁴Kobe University, Kobe, Japan
- ²⁵Kyoto University, Department of Physics, Kyoto, Japan
- ²⁶Lancaster University, Physics Department, Lancaster, United Kingdom
- ²⁷University of Liverpool, Department of Physics, Liverpool, United Kingdom
- ²⁸Louisiana State University, Department of Physics and Astronomy, Baton Rouge, Louisiana, U.S.A.
- ²⁹Université de Lyon, Université Claude Bernard Lyon 1, IPN Lyon (IN2P3), Villeurbanne, France
- ³⁰Miyagi University of Education, Department of Physics, Sendai, Japan
- ³¹National Centre for Nuclear Research, Warsaw, Poland
- ³²State University of New York at Stony Brook, Department of Physics and Astronomy, Stony Brook, New York, U.S.A.
- ³³Okayama University, Department of Physics, Okayama, Japan
- ³⁴Osaka City University, Department of Physics, Osaka, Japan
- ³⁵Oxford University, Department of Physics, Oxford, United Kingdom
- ³⁶UPMC, Université Paris Diderot, CNRS/IN2P3, Laboratoire de
Physique Nucléaire et de Hautes Energies (LPNHE), Paris, France
- ³⁷University of Pittsburgh, Department of Physics and Astronomy, Pittsburgh, Pennsylvania, U.S.A.
- ³⁸Queen Mary University of London, School of Physics and Astronomy, London, United Kingdom
- ³⁹University of Regina, Department of Physics, Regina, Saskatchewan, Canada
- ⁴⁰University of Rochester, Department of Physics and Astronomy, Rochester, New York, U.S.A.
- ⁴¹RWTH Aachen University, III. Physikalisches Institut, Aachen, Germany
- ⁴²University of Sheffield, Department of Physics and Astronomy, Sheffield, United Kingdom
- ⁴³University of Silesia, Institute of Physics, Katowice, Poland
- ⁴⁴STFC, Rutherford Appleton Laboratory, Harwell Oxford, and Daresbury Laboratory, Warrington, United Kingdom
- ⁴⁵University of Tokyo, Department of Physics, Tokyo, Japan
- ⁴⁶University of Tokyo, Institute for Cosmic Ray Research, Kamioka Observatory, Kamioka, Japan
- ⁴⁷University of Tokyo, Institute for Cosmic Ray Research, Research Center for Cosmic Neutrinos, Kashiwa, Japan
- ⁴⁸Tokyo Metropolitan University, Department of Physics, Tokyo, Japan
- ⁴⁹University of Toronto, Department of Physics, Toronto, Ontario, Canada
- ⁵⁰TRIUMF, Vancouver, British Columbia, Canada
- ⁵¹University of Victoria, Department of Physics and Astronomy, Victoria, British Columbia, Canada
- ⁵²University of Warsaw, Faculty of Physics, Warsaw, Poland
- ⁵³Warsaw University of Technology, Institute of Radioelectronics, Warsaw, Poland
- ⁵⁴University of Warwick, Department of Physics, Coventry, United Kingdom
- ⁵⁵University of Washington, Department of Physics, Seattle, Washington, U.S.A.
- ⁵⁶University of Winnipeg, Department of Physics, Winnipeg, Manitoba, Canada
- ⁵⁷Wroclaw University, Faculty of Physics and Astronomy, Wroclaw, Poland
- ⁵⁸York University, Department of Physics and Astronomy, Toronto, Ontario, Canada

(Dated: May 12, 2014)

New data from the T2K neutrino oscillation experiment produce the most precise measurement of the neutrino mixing parameter θ_{23} . Using an off-axis neutrino beam with a peak energy of 0.6 GeV and a data set corresponding to 6.57×10^{20} protons on target, T2K has fit the energy-dependent ν_μ oscillation probability to determine oscillation parameters. The 68% confidence limit

on $\sin^2(\theta_{23})$ is $0.514_{-0.056}^{+0.055}$ (0.511 ± 0.055), assuming normal (inverted) mass hierarchy. The best-fit mass-squared splitting for normal hierarchy is $\Delta m_{32}^2 = (2.51 \pm 0.10) \times 10^{-3} \text{ eV}^2/c^4$ (inverted hierarchy: $\Delta m_{23}^2 = (2.48 \pm 0.10) \times 10^{-3} \text{ eV}^2/c^4$). Adding a model of multinucleon interactions that affect neutrino energy reconstruction is found to produce only small biases in neutrino oscillation parameter extraction at current levels of statistical uncertainty.

PACS numbers: 14.60.Pq,14.60.Lm,13.15+g,29.40.ka

Introduction.—Muon neutrinos oscillate to other flavors with a survival probability approximated by

$$P(\nu_\mu \rightarrow \nu_\mu) \simeq 1 - 4 \cos^2(\theta_{13}) \sin^2(\theta_{23}) [1 - \cos^2(\theta_{13}) \times \sin^2(\theta_{23})] \sin^2(1.267 \Delta m^2 L / E_\nu), \quad (1)$$

where $L(\text{km})$ is the neutrino propagation distance, $E_\nu(\text{GeV})$ is the neutrino energy and $\Delta m^2(\text{eV}^2/c^4)$ is the relevant neutrino mass-squared splitting: $\Delta m_{32}^2 = m_3^2 - m_2^2$ for normal hierarchy (NH), or $\Delta m_{13}^2 = m_1^2 - m_3^2$ for inverted hierarchy (IH). Oscillation occurs because neutrino flavor eigenstates are linear superpositions of mass eigenstates, related by a mixing matrix parametrized by three mixing angles θ_{12} , θ_{23} , θ_{13} , and a CP violating phase δ_{CP} [1]. Previous measurements [2–7] have found $\theta_{23} \approx \pi/4$. There is considerable interest in precise measurements of θ_{23} that can constrain models of neutrino mass generation (see reviews in [8–13]), determine if $\sin^2(2\theta_{23})$ is nonmaximal, and, if so whether θ_{23} is less or greater than $\pi/4$.

In this Letter, we report the world’s most precise measurement of $\sin^2(\theta_{23})$, using more than twice as much data as our previous result [2], as well as new data selections in T2K’s near detector that measure single pion production processes that can mimic the oscillation signal in T2K’s far detector, Super-Kamiokande (SK). We also consider the effects of multiple nucleons ejected in neutrino-nucleus interactions that can cause incorrect neutrino energy estimates and so affect the oscillation probability measurement.

T2K experiment.—The T2K experiment [14] combines (1) a muon neutrino beam line, (2) near detectors, located 280 m downstream of the neutrino production target, that characterize the neutrino beam and constrain the neutrino flux parametrization and cross sections, and (3) the far detector, SK, located at a distance of $L = 295 \text{ km}$ from the target. The neutrino beam axis is 2.5° away from SK, producing a narrow-band beam [15] at the far detector, which reduces back-

grounds from higher-energy neutrino interactions and enhances the sensitivity to θ_{23} . The beam’s peak energy of $E_\nu = 2(1.267 \Delta m^2 L / \pi) \approx 0.6 \text{ GeV}$ corresponds to the first minimum of the ν_μ survival probability at this distance.

A 30 GeV proton beam is extracted in 5 μs spills from the J-PARC main ring, directed toward Kamioka in the primary beam line, and hits a graphite target. Beam monitors measure the beam’s intensity, trajectory, profile, and beam losses. Pions and kaons produced in the target decay into neutrinos in the secondary beam line, which contains three focusing horns and a 96-m-long decay tunnel. This is followed by a beam dump and a set of muon monitors.

The near detector complex [14] contains an on-axis Interactive Neutrino Grid detector (INGRID) [16] and an off-axis magnetized detector, ND280. INGRID provides high-statistics monitoring of the beam intensity, direction, profile, and stability. ND280 is enclosed in a 0.2 T magnet containing a subdetector optimized to measure π^0 s (PØD) [17], three time projection chambers (TPC1,2,3) [18] alternating with two one-tonne fine grained detectors (FGD1,2) [19], and an electromagnetic calorimeter [20] that surrounds the central detectors. A side muon range detector [21] identifies muons that exit or stop in the magnet steel.

The SK water-Cherenkov far detector [22] has a 22.5 kt fiducial volume within a cylindrical inner detector (ID) with 11 129 inward-facing 20" phototubes. Surrounding the ID is a 2 meter wide outer detector with 1885 outward-facing 8" phototubes. A global positioning system with <150 ns precision synchronizes the timing between SK events and the J-PARC beam spill.

Data were collected during four periods: January-June 2010, November 2010-March 2011, January-June 2012, and October 2012-May 2013. The proton beam power on the target steadily increased, reaching 220 kW with a world record of 1.2×10^{14} protons on target (POT) per spill. The total neutrino beam exposure on the SK detector was 6.57×10^{20} POT.

Analysis strategy.—The analysis determines oscillation parameters by comparing the observed and predicted ν_μ interaction rates and energy spectra at the far detector. These predictions depend on the oscillation parameters, the incident neutrino flux, neutrino interaction cross sections, and the detector response.

A measurement of ν_μ charged current (CC) events in ND280 is used to tune both the initial flux estimates and parameters of the neutrino interaction models. The measurement also estimates the uncertainties in the predicted neutrino spectrum at the far detector. In this

* also at J-PARC, Tokai, Japan

† also at Institute of Particle Physics, Canada

‡ affiliated member at Kavli IPMU (WPI), the University of Tokyo, Japan

§ also at Moscow Institute of Physics and Technology and National Research Nuclear University "MEPhI", Moscow, Russia

¶ also at JINR, Dubna, Russia

** deceased

†† also at BMCC/CUNY, Science Department, New York, New York, U.S.A.

new analysis, the ND280 measurement provides better constraints on the flux and interaction model parameters by using improved event selections, reconstruction, and higher ND280 statistics. This improvement was achieved by dividing CC events into three categories based on the number of pions in the final state.

At SK, the rate and energy spectrum of ν_μ charged current quasielastic (CCQE) events are used to determine the oscillation parameters through a maximum likelihood fit. The fit accounts for uncertainties in the predicted spectrum not only from the ND280-constrained flux and interaction models but also SK detector selection efficiencies, final state interactions (FSI) inside the nucleus, and secondary pion interactions (SI) in the detector material.

Initial neutrino flux model.—Detailed simulations of hadron production and secondary interactions for primary beam protons striking T2K’s graphite target predict the neutrino fluxes at ND280 and SK [15]. The simulation is tuned to hadron production data such as those from NA61/SHINE for 30 GeV protons on graphite [23]. Pions and kaons produced outside the experimentally measured phase space are modeled using FLUKA2008 [24]. The GEANT3-based simulations model the horns’ magnetic field, particle interactions in the horns and decay region, and neutrino production from hadron decays. Flux uncertainties are 10%-20%, varying with energy, and are dominated by hadron production uncertainties. Full covariances between all SK and ND280 energy bins and ν flavors are calculated [25].

Neutrino interaction simulations and cross section Parameters.—The NEUT Monte Carlo (MC) generator [26] is used to simulate neutrino interactions in T2K’s detectors. External data, especially from the MiniBooNE experiment [27], set the initial parameters and their uncertainties subsequently used in the fit to the ND280 data [25]. Neutrino interaction parameters fall into two categories: parameters common between ND280 and SK, and independent parameters affecting interactions at only one detector. The common parameters include the axial masses for CCQE and resonant pion production, as well as 5 energy-dependent normalizations; these are included in the fit to the ND280 data, as discussed in the next section. Since the ND280 target is mainly carbon while SK’s target is mainly oxygen, additional independent parameters are required which describe the nuclear model used for CCQE simulation (Fermi momentum, binding energy and spectral function modeling). Five additional cross section parameters relate to pion production, the neutral current (NC) cross section, the ν_e/ν_μ CC cross section ratio, and the $\nu/\bar{\nu}$ CC cross section ratio. These independent cross section uncertainties (11 parameters) produce a 4.9% fractional error in the expected number of SK events (see Table I). Multinucleon interactions are thought to lead to an enhancement of the low-energy cross section [28–32] and have been modeled with a variety of approaches [33–37]. These effects, not currently included in NEUT, may affect the oscillation parameter determination [38–43]. The penultimate

section presents a study of this potential bias.

ND280 measurements and fits.—The neutrino flux, spectrum, and cross section parameters are constrained using ν_μ CC interactions in ND280. We select the highest-momentum negatively charged track entering TPC2 with a vertex inside FGD1’s fiducial volume and an energy loss in TPC2 consistent with a muon. Events originating from interactions in upstream detectors are vetoed by excluding events with a track in TPC1, which is upstream of FGD1.

The ND280 analysis includes many improvements [44] over T2K’s previous ν_μ disappearance measurement [2], and used a data set with 5.90×10^{20} POT. The selected CC candidate events are now divided into three samples: CC-0 π , with no identified pions; CC-1 π^+ , with exactly one π^+ and no π^- or π^0 ; and CC-other, with all the other CC events. The CC-0 π are dominated by CCQE interactions; CC-1 π^+ are dominated by CC resonant pion production; and CC-other, a mixture of resonant production and deep inelastic scattering having final states with π^0 ’s, π^- ’s, or multiple pions.

A π^+ is identified in one of three ways: an FGD+TPC track with positive curvature and a TPC charge deposition consistent with a pion, an FGD-contained track with a charge deposition consistent with a pion, or a delayed energy deposit due to a decay electron from stopped $\pi^+ \rightarrow \mu^+$ in the FGD. A π^- is tagged only by a negatively curved FGD+TPC track. A π^0 is identified from a track in the TPC with a charge deposition consistent with an electron from a γ conversion.

The dominant sources of uncertainty are events occurring outside the FGD fiducial volume and pion reinteractions in the detector.

We fit these three samples for 25 parameters describing the beam flux in bins of energy and neutrino type at ND280. These parameters strongly correlate with flux parameters at SK. We also fit for 19 cross section parameters and for nuisance parameters describing correlated detector uncertainties of the data bins (10 momentum \times 7 angle bins for each sample).

We observe 17 369, 4047, and 4173 data events in the CC-0 π , CC-1 π^+ , and CC-other samples, respectively. Using the best-fit parameters, the simulated numbers of events are 17 352, 4110, and 4119 for the CC-0 π , CC-1 π^+ , and CC-other samples. Figure 1 shows distributions of the muon momentum and angle relative to the beam direction for the CC-0 π sample and the improvement in data and MC agreement when using the best-fit parameters. The fit uses the neutrino interaction model to extrapolate ND280 measurements, primarily covering $\cos(\theta_\mu) > 0.5$, over SK’s 4π angular acceptance.

The fit gives estimates for 16 beam flux parameters at SK, the seven common cross section parameters, and their covariance. Using the ND280 data reduces the uncertainty on the expected number of events at SK due to these parameters from 21.6% to 2.7%.

SK measurements.—An enriched sample of ν_μ CCQE events, occurring within $-2 \mu\text{s}$ to $+10 \mu\text{s}$ of the ex-

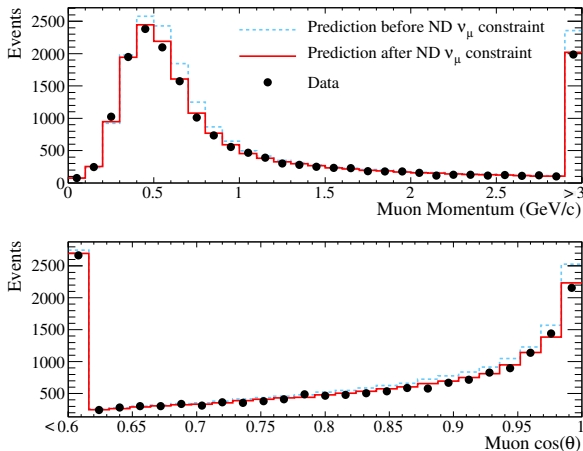


FIG. 1. The momentum and angular distributions for muons in ND280’s CC-0 π selection. The predicted distributions before and after the ND280 fit are overlaid on both figures.

pected neutrino arrival time, is selected in SK. We require low activity in the outer detector to reduce entering backgrounds. We also require: visible energy > 30 MeV, exactly one reconstructed Cherenkov ring, μ -like particle identification, reconstructed muon momentum > 200 MeV, and ≤ 1 reconstructed decay electron. The reconstructed vertex must be in the fiducial volume (at least 2 m away from the ID walls) and we reject “flasher” events (produced by intermittent light emission inside phototubes). More details about the SK event selection and reconstruction are found in [22].

The neutrino energy for each event is calculated under the quasielastic assumption as in [2] using an average binding energy of 27 MeV for nucleons in ^{16}O . The E_{reco} distribution of the 120 selected events is shown in Fig. 2. The MC expectation without oscillations is 446.0 ± 22.5 (syst.) events, of which 81.0% are $\nu_{\mu} + \bar{\nu}_{\mu}$ CCQE, 17.5% are $\nu_{\mu} + \bar{\nu}_{\mu}$ CC non-QE, 1.5% are NC and 0.02% are $\nu_e + \bar{\nu}_e$ CC. The expected resolution in reconstructed energy for $\nu_{\mu} + \bar{\nu}_{\mu}$ CCQE events near the oscillation maximum is ~ 0.1 GeV.

Systematic uncertainties in the analysis are evaluated with atmospheric neutrinos, cosmic-ray muons, and their decay electrons. Correlated selection efficiency parameters are assigned for six event categories: $\nu_{\mu} + \bar{\nu}_{\mu}$ CCQE in three energy bins, $\nu_{\mu} + \bar{\nu}_{\mu}$ CC non-QE, $\nu_e + \bar{\nu}_e$ CC, and NC events. An energy scale uncertainty of 2.4% comes from comparing reconstructed momenta in data and MC for cosmic-ray stopping muons and associated decay electrons, and from comparing reconstructed invariant mass in data and MC simulations for π^0 ’s produced by atmospheric neutrinos. Systematic uncertainties in pion interactions in the target nucleus (FSI) and SK detector (SI) are evaluated by varying pion interaction probabilities in the NEUT cascade model. These SK detector and FSI+SI uncertainties produce a 5.6% fractional error in the expected number of SK events (see Table I).

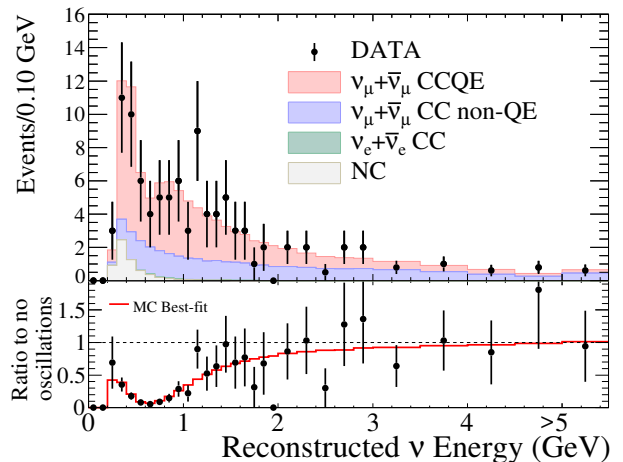


FIG. 2. Reconstructed energy spectrum for single-ring μ -like SK events. Top: The observed spectrum and expected spectrum with interaction modes for the T2K best fit. Bottom: The ratio of the observed spectrum (points) to the no-oscillation hypothesis, and the best oscillation fit (solid).

Source of uncertainty (number of parameters)	$\delta n_{\text{SK}}^{\text{exp}} / n_{\text{SK}}^{\text{exp}}$
ND280-independent cross section (11)	4.9%
Flux and ND280-common cross section (23)	2.7%
SK detector and FSI+SI systematics (7)	5.6%
$\sin^2(\theta_{13})$, $\sin^2(\theta_{12})$, Δm_{21}^2 , δ_{CP} (4)	0.2%
Total (45)	8.1%

TABLE I. Effect of 1σ systematic parameter variation on the number of 1-ring μ -like events, computed for oscillations with $\sin^2(\theta_{23}) = 0.500$ and $|\Delta m_{32}^2| = 2.40 \times 10^{-3} \text{ eV}^2/c^4$.

Oscillation fits.—We estimate oscillation parameters using an unbinned maximum likelihood fit to the SK spectrum for the parameters $\sin^2(\theta_{23})$ and either Δm_{32}^2 or Δm_{13}^2 for the normal and inverted mass hierarchies respectively, and all 45 systematic parameters. The fit uses 73 unequal-width energy bins, and interpolates the spectrum between bins. Oscillation probabilities are calculated using the full three-flavor oscillation framework. Matter effects are included with an Earth density of $\rho = 2.6 \text{ g/cm}^3$ [45], δ_{CP} is unconstrained in the range $[-\pi, \pi]$, and other oscillation parameters are fit with constraints $\sin^2(\theta_{13}) = 0.0251 \pm 0.0035$, $\sin^2(\theta_{12}) = 0.312 \pm 0.016$, and $\Delta m_{21}^2 = (7.50 \pm 0.20) \times 10^{-5} \text{ eV}^2/c^4$ [46]. Figure 2 shows the best-fit neutrino energy spectrum. The point estimates of the 45 nuisance parameters are all within 0.25 standard deviations of their prior values.

Two-dimensional confidence regions in the oscillation parameters are constructed using the Feldman-Cousins method [47], with systematics incorporated using the Cousins-Highland method [48]. Figure 3 shows 68% and 90% confidence regions for the oscillation parameters for both normal and inverted hierarchies. The 68% and 90% expected sensitivity curves are each 0.04 wider in $\sin^2(\theta_{23})$ than these contours. An alternative analy-

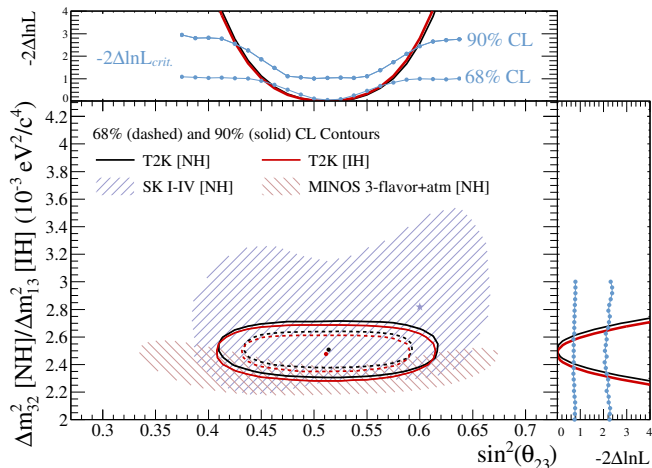


FIG. 3. The 68% and 90% C.L. confidence regions for $\sin^2(\theta_{23})$ and Δm_{32}^2 (NH) or Δm_{13}^2 (IH). The SK [49] and MINOS [7] 90% C.L. regions for NH are shown for comparison. T2K’s 1D profile likelihoods for each oscillation parameter separately are also shown at the top and right overlaid with light blue lines and points representing the 1D $-2\Delta \ln \mathcal{L}_{\text{critical}}$ values for NH at 68% and 90% C.L.

sis employing a binned likelihood ratio gave consistent results. Also shown are 90% confidence regions from other recent experimental results. Statistical uncertainties dominate T2K’s error budget.

We calculate one-dimensional (1D) limits using a new method inspired by Feldman-Cousins [47] and Cousins-Highland [48] that marginalizes over the second oscillation parameter. Toy experiments are used to calculate $-2\Delta \ln \mathcal{L}_{\text{critical}}$ values, above which a parameter value is excluded, for each value of $\sin^2(\theta_{23})$. These toy experiments draw values for Δm_{32}^2 or Δm_{13}^2 in proportion to the likelihood for fixed $\sin^2(\theta_{23})$, marginalized over systematic parameters. The toy experiments draw values of the 45 systematic parameters from either Gaussian or uniform distributions. We generate Δm_{32}^2 or Δm_{13}^2 limits with the same procedure. Figure 3 shows the 1D profile likelihoods for both mass hierarchies, with the $-2\Delta \ln \mathcal{L}_{\text{critical}}$ MC estimates for NH.

The 1D 68% confidence intervals are $\sin^2(\theta_{23}) = 0.514_{-0.056}^{+0.055}$ (0.511 ± 0.055) and $\Delta m_{32}^2 = 2.51 \pm 0.10$ ($\Delta m_{13}^2 = 2.48 \pm 0.10$) $\times 10^{-3} \text{ eV}^2/c^4$ for the NH (IH). The best fit corresponds to the maximal possible disappearance probability for the three-flavor formula.

Effects of multinucleon interactions.—Inspired by more precise measurements of neutrino-nucleus scattering [50–53], recent theoretical work suggests that neutrino interactions involving multinucleon mechanisms may be a significant part of the cross section in T2K’s energy range and might introduce a bias on the oscillation parameters as large as a few percent [28–43]. We are the first oscillation experiment to consider the potential bias introduced by multinucleon interactions including potential cancellation from measurements at the near

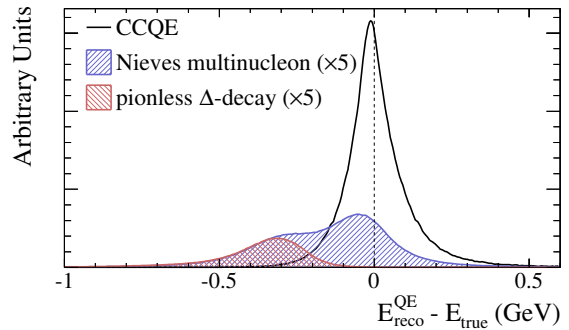


FIG. 4. The difference between the reconstructed energy assuming QE kinematics and the true neutrino energy. True QE events with energies below 1.5 GeV show little bias while multinucleon events based on [43] and NEUT pionless Δ decay (shown scaled up by a factor of 5) are biased towards lower energies.

detector. At T2K beam energies most interactions produce final-state nucleons below SK’s Cherenkov threshold, making multinucleon interactions indistinguishable from quasielastic (QE) interactions. Even if the additional nucleon does not leave the nucleus, the multinucleon mechanism alters the kinematics of the outgoing lepton, distorting the reconstructed neutrino energy which assumes QE kinematics (see Fig. 4) in addition to increasing the overall QE-like event rate.

The T2K neutrino interaction generator, NEUT, includes an effective model (pionless Δ decay) that models some but not all of the expected multinucleon cross section. In order to evaluate the possible effect on the oscillation analysis, we perform a Monte Carlo study where the existing effective model is replaced with a multinucleon prediction based on the work of Nieves [43] going up to 1.5 GeV in energy. We used this modified simulation to make ND280 and SK fake data sets with randomly chosen systematic uncertainties but without statistical fluctuations, and performed oscillation analyses as described above on each of them, allowing ND280 fake data to renormalize the SK prediction. The mean biases in the determined oscillation parameters are $< 1\%$ for the ensemble, though the $\sin^2(\theta_{23})$ biases showed a 3.5% rms spread.

Conclusions.—The measurement of $\sin^2(\theta_{23}) = 0.514_{-0.056}^{+0.055}$ (0.511 ± 0.055) for NH (IH) is consistent with maximal mixing and is more precise than previous measurements. The best-fit mass-squared splitting is $\Delta m_{32}^2 = 2.51 \pm 0.10$ (IH: $\Delta m_{13}^2 = 2.48 \pm 0.10$) $\times 10^{-3} \text{ eV}^2/c^4$. Possible multinucleon knockout in neutrino-nucleus interactions produces a small bias in the fitted oscillation parameters and is not a significant uncertainty source at present precision.

We thank the J-PARC staff for superb accelerator performance and the CERN NA61 collaboration for providing valuable particle production data. We acknowledge the support of MEXT, Japan; NSERC, NRC, and

CFI, Canada; CEA and CNRS/IN2P3, France; DFG, Germany; INFN, Italy; National Science Centre (NCN), Poland; RAS, RFBR, and MES, Russia; MICINN and CPAN, Spain; SNSF and SER, Switzerland; STFC, UK; and DOE, USA. We also thank CERN for the UA1/NOMAD magnet, DESY for the HERA-B magnet mover system, NII for SINET4, the WestGrid and

SciNet consortia in Compute Canada, GridPP, UK, and the University of Oxford Advanced Research Computing (ARC) facility. In addition participation of individual researchers and institutions has been further supported by funds from: ERC (FP7), EU; JSPS, Japan; Royal Society, UK; DOE Early Career program, USA.

-
- [1] B. Pontecorvo, *JETP* **6**, 429 (1957); **7**, 172 (1958); **26**, 984 (1968); Z. Maki, M. Nakagawa, and S. Sakata, *Prog. Theor. Phys.* **28**, 870 (1962).
- [2] K. Abe et al. (T2K Collaboration), *Phys. Rev. Lett.* **111**, 211803 (2013).
- [3] K. Abe et al. (The T2K Collaboration), *Phys. Rev. D* **85**, 031103 (2012).
- [4] R. Wendell et al. (The Super-Kamiokande Collaboration), *Phys. Rev. D* **81**, 092004 (2010).
- [5] P. Adamson et al. (MINOS Collaboration), *Phys. Rev. Lett.* **108**, 191801 (2012).
- [6] P. Adamson et al. (MINOS Collaboration), *Phys.Rev.Lett.* **110**, 251801 (2013), arXiv:1304.6335 [hep-ex].
- [7] P. Adamson et al. (MINOS Collaboration), submitted to *Phys. Rev. Lett.* (2014), arXiv:1403.0867 [hep-ex].
- [8] S. F. King and C. Luhn, *Rept.Prog.Phys.* **76**, 056201 (2013), arXiv:1301.1340 [hep-ph].
- [9] C. H. Albright, A. Dueck, and W. Rodejohann, *Eur.Phys.J.* **C70**, 1099 (2010), arXiv:1004.2798 [hep-ph].
- [10] G. Altarelli and F. Feruglio, *Rev.Mod.Phys.* **82**, 2701 (2010), arXiv:1002.0211 [hep-ph].
- [11] H. Ishimori, T. Kobayashi, H. Ohki, Y. Shimizu, H. Okada, et al., *Prog.Theor.Phys.Suppl.* **183**, 1 (2010), arXiv:1003.3552 [hep-th].
- [12] C. H. Albright and M.-C. Chen, *Phys.Rev.* **D74**, 113006 (2006), arXiv:hep-ph/0608137 [hep-ph].
- [13] R. Mohapatra and A. Smirnov, *Ann.Rev.Nucl.Part.Sci.* **56**, 569 (2006), arXiv:hep-ph/0603118 [hep-ph].
- [14] K. Abe et al. (T2K Collaboration), *Nucl. Instrum. Methods* **A659**, 106 (2011), see Figure 16 for a schematic diagram of the ND280 detector.
- [15] K. Abe et al. (T2K Collaboration), *Phys. Rev. D* **87**, 012001 (2013), see the predicted flux at SK reweighted with the NA61/SHINE measurement in Fig. 39 and the neutrino events per POT as measured by the INGRID sub-detector in Fig. 12.
- [16] K. Abe et al. (T2K Collaboration), *Nucl. Instrum. Methods* **A694**, 211 (2012).
- [17] S. Assylbekov et al. (T2K ND280 P0D Collaboration), *Nucl. Instrum. Methods* **A686**, 48 (2012).
- [18] N. Abgrall et al. (T2K ND280 TPC Collaboration), *Nucl. Instrum. Methods* **A637**, 25 (2011).
- [19] P. Amaudruz et al. (T2K ND280 FGD Collaboration), *Nucl. Instrum. Methods* **A696**, 1 (2012).
- [20] D. Allan et al., *J. Instrum.* **8**, P10019 (2013), arXiv:1308.3445 [physics.ins-det].
- [21] S. Aoki et al. (T2K ND280 SMRD Collaboration), *Nucl. Instrum. Methods* **A698**, 135 (2013), arXiv:1206.3553 [physics.ins-det].
- [22] Y. Ashie et al. (Super-Kamiokande Collaboration), *Phys. Rev. D* **71**, 112005 (2005).
- [23] N. Abgrall et al. (NA61/SHINE Collaboration), *Phys. Rev. C* **84**, 034604 (2011); *Phys. Rev. C* **85**, 035210 (2012).
- [24] A. Ferrari, P. R. Sala, A. Fasso, and J. Ranft, CERN-2005-010, SLAC-R-773, INFN-TC-05-11 (2005); G. Battistoni, S. Muraro, P. R. Sala, F. Cerutti, A. Ferrari, et al., *AIP Conf.Proc.* **896**, 31 (2007).
- [25] K. Abe et al. (T2K Collaboration), *Phys.Rev.* **D88**, 032002 (2013), see sections IV and V on the neutrino interaction model and the neutrino flux model, arXiv:1304.0841 [hep-ex].
- [26] Y. Hayato, *Acta Phys. Pol. B* **40**, 2477 (2009).
- [27] A. A. Aguilar-Arevalo et al. (MiniBooNE Collaboration), *Phys. Rev. D* **81**, 092005 (2010).
- [28] J. Marteau, *Eur.Phys.J.* **A5**, 183 (1999), arXiv:hep-ph/9902210 [hep-ph].
- [29] M. Martini, M. Ericson, G. Chanfray, and J. Marteau, *Phys. Rev. C* **80**, 065501 (2009).
- [30] J. Carlson, J. Jourdan, R. Schiavilla, and I. Sick, *Phys.Rev.* **C65**, 024002 (2002), arXiv:nucl-th/0106047 [nucl-th].
- [31] G. Shen, L. Marcucci, J. Carlson, S. Gandolfi, and R. Schiavilla, *Phys.Rev.* **C86**, 035503 (2012), arXiv:1205.4337 [nucl-th].
- [32] A. Bodek, H. Budd, and M. Christy, *Eur. Phys. J. C* **71**, 1726 (2011).
- [33] M. Martini, M. Ericson, G. Chanfray, and J. Marteau, *Phys. Rev. C* **81**, 045502 (2010).
- [34] M. Martini and M. Ericson, *Phys.Rev.* **C87**, 065501 (2013), arXiv:1303.7199 [nucl-th].
- [35] J. Nieves, M. Valverde, and M. Vicente Vacas, *Phys.Rev.* **C73**, 025504 (2006), arXiv:hep-ph/0511204 [hep-ph].
- [36] O. Benhar, A. Fabrocini, S. Fantoni, and I. Sick, *Nucl.Phys.* **A579**, 493 (1994).
- [37] R. Gran, J. Nieves, F. Sanchez, and M. J. Vicente Vacas, *Phys.Rev.* **D88**, 113007 (2013), arXiv:1307.8105 [hep-ph].
- [38] J. Nieves, F. Sanchez, I. Ruiz Simo, and M. Vicente Vacas, *Phys.Rev.* **D85**, 113008 (2012), arXiv:1204.5404 [hep-ph].
- [39] O. Lalakulich, U. Mosel, and K. Gallmeister, *Phys.Rev. C* **86**, 054606 (2012), arXiv:1208.3678 [nucl-th].
- [40] M. Martini, M. Ericson, and G. Chanfray, *Phys.Rev.D* **85**, 093012 (2012), arXiv:1202.4745 [hep-ph].
- [41] M. Martini, M. Ericson, and G. Chanfray, *Phys.Rev.D* **87**, 013009 (2013), arXiv:1211.1523v2 [hep-ph].
- [42] D. Meloni and M. Martini, *Phys.Lett.B* **716**, 186 (2012), arXiv:1203.3335 [hep-ex].
- [43] J. Nieves, I. R. Simo, and M. Vicente Vacas, *Phys.Lett.B* **707**, 72 (2012).
- [44] K. Abe et al. (T2K Collaboration), *Phys.Rev.Lett.* **112**, 061802 (2014), arXiv:1311.4750 [hep-ex].

- [45] K. Hagiwara, N. Okamura, and K.-i. Senda, *JHEP* **1109**, 082 (2011), arXiv:1107.5857 [hep-ph].
- [46] J. Beringer *et al.* (PDG), *Phys.Rev.* **D86**, 010001 (2012, and 2013 partial update for the 2014 edition).
- [47] G. J. Feldman and R. D. Cousins, *Phys. Rev. D* **57**, 3873 (1998).
- [48] R. D. Cousins and V. L. Highland, *Nucl. Instrum. Methods* **A320**, 331 (1992).
- [49] A. Himmel (Super-Kamiokande Collaboration), 7th Intl. Conf. on Interconnection between Particle Physics & Cosmology (PPC 2013) (2013), arXiv:1310.6677 [hep-ex].
- [50] A. Aguilar-Arevalo *et al.* (MiniBooNE Collaboration), *Phys.Rev.Lett.* **100**, 032301 (2008), arXiv:0706.0926 [hep-ex].
- [51] A. Aguilar-Arevalo *et al.* (MiniBooNE Collaboration), *Phys.Rev.* **D88**, 032001 (2013), arXiv:1301.7067 [hep-ex].
- [52] L. Fields *et al.* (MINERvA Collaboration), *Phys.Rev.Lett.* **111**, 022501 (2013), arXiv:1305.2234 [hep-ex].
- [53] G. Fiorentini *et al.* (MINERvA Collaboration), *Phys.Rev.Lett.* **111**, 022502 (2013), arXiv:1305.2243 [hep-ex].